ENCAPSULANT FREE-SURFACES AND INTERFACES: CRITICAL PARAMETERS IN CONTROLLING CELL CORROSION*

G. Mon**, L. Wen**, R. Ross, Jr.***

Jet Propulsion Laboratory
California Institute of Technology
Pasadena, CA

ABSTRACT

We present some results of studying the interaction of moisture with photovoltaic (PV) modules and custom-built test coupons in both laboratory and outdoor ambient environments. We measured module cell-to-frame leakage currents, encapsulant bulk and surface currents, glass surface currents, and encapsulant/glass interface currents as functions of temperature and humidity. Using a computer model of inter-electrode conduction, we delineate preferential conduction paths in PVB- and EVA-encapsulated modules. In comparing the results of field and laboratory test environments on identical samples, we note and comment upon the greater severity of the outdoor environment. We conclude with a discussion of several aspects of water-module interaction, including design strategies and continuing research aims.

BACKGROUND

A particular performance degradation mode that has been extensively documented is electrochemical corrosion (1-4). Voltage differences between two electrified cells within a module, or between an electrified cell and a grounded frame, drive chemical oxidation and reduction reactions at the cell/encapsulant and the frame/encapsulant interfaces and cause ionic ("leakage") currents to flow between these electrified module parts. A schematic depiction of this process is shown in Fig. 1.

Leakage current, which is the rate of inter-electrode ionic charge transfer, is a measure of the electrochemical reaction rate and can be modelled as an Arrhenius temperature/rate process (log current inversely proportional to reciprocal absolute temperature) with a rate doubling for approximately every 10°C increase in temperature (5). Its level is determined by the impressed voltage, the geometric arrangement of the module components, and the effective ionic conductivity,

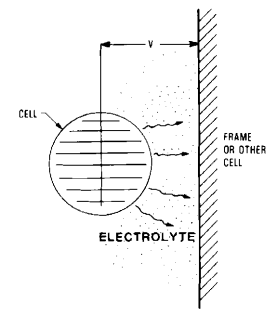

Fig. 1. Schematic of Corrosion

which depends upon the environmentally sensitive dielectric and water sorption properties of the encapsulant.

The encapsulant plays a key role in module electrochemical processes; its selection affords the major opportunity for controlling ionic charge transfer rates in photovoltaic modules. It serves as the (solid state) electrolyte in electrode interactions and is the medium through and along which dissolved metallization ions are transported. The dielectric properties of the polymeric compound determine the ease with which metallization ions dissolve. Its conductivity properties and indigenous ionizable species concentrations determine the inter-electrode ion transfer magnitudes. The values of these fundamentally important encapsulant properties are strongly affected by the encapsulant temperature and moisture content. Hence module ionic charge transfer rates will depend, in a complex way, on the environmental temperature and water vapor partial pressure variations and on the water sorption and diffusion characteristics of the polymer.

The interplay of moisture with polymer materials--i.e., the module encapsulant--is more

---

* This paper presents the results of one phase of research conducted at the Jet Propulsion Laboratory, California Institute of Technology, for the U.S. Department of Energy, through an agreement with the National Aeronautics and Space Administration.

** Member of the Technical Staff, Photovoltaic Engineering Group, System Integration Section.

*** Supervisor, Photovoltaic Engineering Group, System Integration Section.

Proceedings of the 19th IEEE Photovoltaic Specialists Conference
New Orleans, Louisiana, May 4-8, 1987
pp. 1215-1221.

involved (6,7) and hence less well understood than are temperature-rate relationships. Whereas all parts of a PV module are at approximately the same temperature ($\pm 3^{o}C$), the moisture level can vary by orders of magnitude from module surface to module interior. This greatly complicates the calculation of moisture effects because the moisture level must be specifically computed for the exact site of the governing reaction. Quantifying the reaction rates expected under varying field conditions (temperature, relative humidity, dew, rain, etc.) requires complex transient models of the modules' spatial moisture sorption together with detailed knowledge of the leakage current dependency on this moisture level and distribution.

In this paper we present data that may serve as a basis for quantitative studies of the water/module interaction problem. We present sorption measurement data for the encapsulants PVB and EVA. We present Arrhenius activation energy constants for bulk conduction in these encapsulant materials, together with plots of bulk and surface conductivity of EVA and PVB, surface conductivity of a borosilicate and a soda-lime glass, and interface conductivities of these encapsulant/glass composites. These data were used in a computerized simulation of two-dimensional conduction to study ionic conduction characteristics of PVB- and EVA-encapsulated modules. Laboratory and field surface, bulk, and interface data on the same test coupons are compared; these data reveal that the "real world" environment is more severe than generally applied laboratory temperature/humidity environments. The consequences of these data will be discussed.

SORPTION

Sorption data were acquired utilizing a Cahn Balance having microgram resolution. From one arm of the beam balance the sample, typically a sheet of polymer, is suspended in a Blue M environmental chamber. The other arm sports counterweights suspended in an unchanging environment. The chamber environment can be controlled over the ranges 10% - 100% relative humidity (RH) and $20^{o}C$ - $85^{o}C$.

Sorption equilibrium isotherms, based upon data collected at JPL from pristine PVB and EVA samples, are presented in Figure 2. The isotherms account for both surface and bulk water. It is seen that PVB is considerably more sorbant than EVA.

This sorption data was acquired on polymer sheets offering large areal exposure to the applied environment. The data may be applicable to unglassed modules but perhaps not to glass-polymer-glass modules which offer limited polymer exposure (generally along a gasketed lineal perimeter) to the environment.

IONIC CONDUCTION

Water within a polymer and on its surface that is available to participate in the ionic conduction process does so by providing a medium in which ionization can readily occur. The high

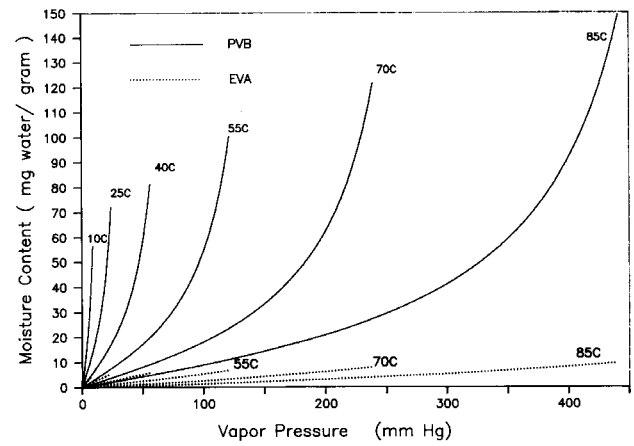

Fig. 2. Water Sorption Isotherms for PVB and EVA

relative permittivity of water (Z_W = 82) provides 10 to 30 times more ionizing power than do typical dry PV module polymer encapsulants (Z_{EVA} = 3.8, Z_{PVB} = 10.7). Thus sorbed water enhances ionization within a polymer by increasing its permittivity.

Analytical Expressions

Semi-empirical equations having some theoretical basis (8,9) have been utilized to relate the dependency of ionic conduction upon temperature, sorbed moisture content, and material permittivities. We use these equations and further develop them to provide analytical expressions against which to compare experimental measurements and to serve as a basis for model analysis of overall PV module conduction processes:

$$k = M_o \exp[-E/RT], \quad E = U_o/2Z \qquad \ldots(1)$$

where

- k = ionic conductivity, $(\text{ohm-cm})^{-1}$
- M_o = scale constant, $(\text{ohm-cm})^{-1}$
- R = gas constant, 1.987 cal/mole-^{o}K
- T = temperature, ^{o}K
- E = activation energy, cal/mole (the energy required to ionize one mole of bound ion in a medium)
- U_o = dissociation energy, cal/mole (the energy required to ionize one mole of bound ion in-vacuum)
- Z = relative permittivity of polymer medium

Bulk Conductivity. We model the bulk permittivity of a polymer/water composite as

$$Z = Z_p(Z_W/Z_p)^C \qquad \ldots(2)$$

where C is the volume fraction of water in the composite and the subscripts "p" and "w" refer to "polymer" and "water", respectively. This formula derives from an expression by Hartshorn (9) modified to apply to a polymer with specific gravity near unity and having a small water concentration.

When Eqn. 2 is substituted into Eqn. 1, we obtain

$$k_V = M_0 \exp[-(E_V/RT)(Z_p/Z_w)^C] \quad ...(3)$$

where $E_V = U_0/2Z_p$ is the activation energy for the dry state, $C = 0$. If a material suffers hygro-thermal degradation, its sorption capacity will generally increase. To account for degradation, we replace C in Eqns. 2 and 3 with hC. The degradation factor h multiplies the water concentration C over what it would be in the non-degraded material for equivalent exposure conditions.

Surface Conductivity. For water on a polymer surface, we adopt the expression

$$Z = Z_p \ (V_p + V_w \ Z_p/Z_w)^{-1} \quad ...(4)$$

where V_p and V_w are the polymer and water volume ratios relative volume of the composite surface conduction layer. Substituting Eqn. 4 into Eqn. 1 gives

$$k_S = M_S \exp[-(E_S/RT)\{1-V_w(1-Z_p/Z_w)\}] \quad ...(5)$$

For surface conductivity we make the additional distinction that $V_w = yr$, where y is the fraction of the surface covered with moisture and r is the water volume ratio of the covered sites, assumed to be equal to the ambient relative humidity for steady state exposure conditions. For polymer surfaces, experimental conduction data can be fitted with y-values near 1, but for glass surfaces, a better fit is obtained with y about 0.1.

Interface Conductivity.

We invoke superposition to model the ionic conductivity of a polymer/glass interface:

$$k_I = k_g + k_p \quad ...(6)$$

A superposition model may be valid if, for example, the two surfaces strongly interact or if adhesive binders or primers (10) are used to promote coupling.

Experimental Results: Laboratory

Activation Energies. Arrhenius plots for "dry" PVB and EVA are presented in Fig. 3. The data groupings reflect different sample design and fabrication processes, but despite considerable differences in sample exposure histories, the activation energies have remained relatively constant at E_V = 17.1 kcal/mole for PVB and E_V = 13.6 kcal/mole for EVA.

Bulk Conductivities. Bulk equilibrium ionic conductivity data for pristine PVB and EVA are presented in Fig. 4. The superposed curves are generated using Eqn. 3 with $M_V = 15$ (ohm cm)$^{-1}$ and h = 1 for the PVB data, and $M_V = 0.000224$ (ohm-cm)$^{-1}$ and h = 2.31. The degradation factor h = 2.31 giving the "best" fit for the EVA data may imply that the EVA used to obtain this data may have been more sorbant than that used to obtain the sorption data in Fig. 2. EVA exposed 45 days to an 85°C/85%RH environment exhibited sorption capacities more than twice those indicated in Fig. 2.

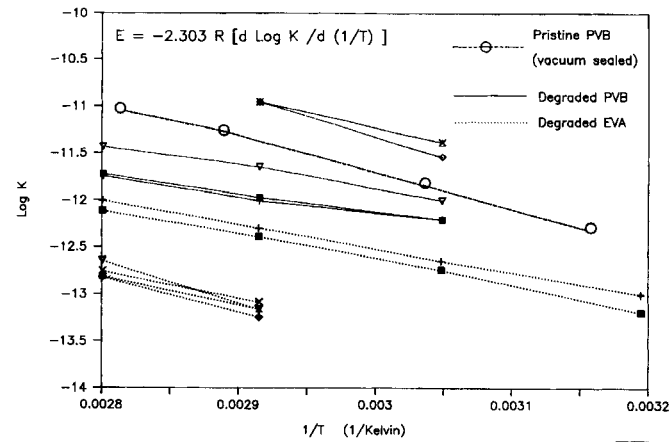

Fig. 3. Arrhenius Plots for Bulk Ionic Conduction in Dry PVB and EVA

The data of Fig. 4 indicates that PVB is more conductive than EVA by three orders of magnitude and considerably more sensitive to temperature and humidity variations (1). This is attributed in part to the fact that PVB has a considerably higher ionizable species content than EVA, which does not contain added plasticizer and crosslinks in curing.

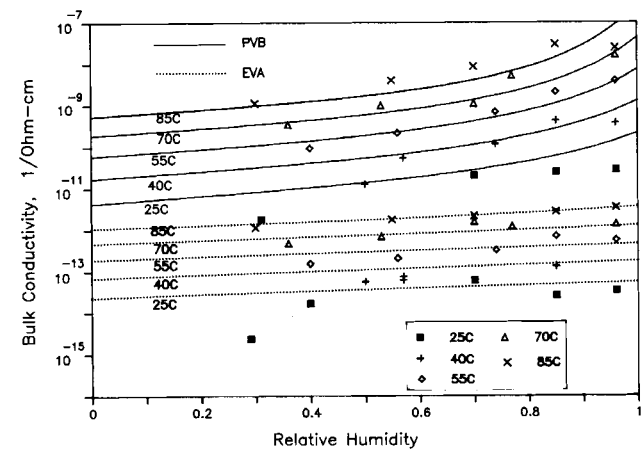

Fig. 4. Bulk Conductivity of PVB and EVA

Surface Conductivities. The raw PVB and EVA surface and interface conductivity data contain bulk contributions. To permit division of this data into bulk, surface, and interfacial components, a multi-nodal network model (11), which outputs voltage at each node and current flow between adjacent nodes, was constructed to simulate the conduction paths in the measurement samples.

The PVB and EVA surface conductivity data, with bulk contributions excluded, are presented in Fig. 5. The superposed curves are generated using Eqn. 5 with $M_S = 1.26E^{-7}$ ohm^{-1}, E_S = 12.45 kcal/mole, and y = 1 for PVB, and with $M_S = 1.7E^{-12}$ ohm^{-1}, E_S = 6.32 kcal/mole, and y = 1 for EVA, respectively. Compared to bulk conductivity values, surface conductivity values are relatively insensitive to temperature variations but are very responsive to relative humidity variations.

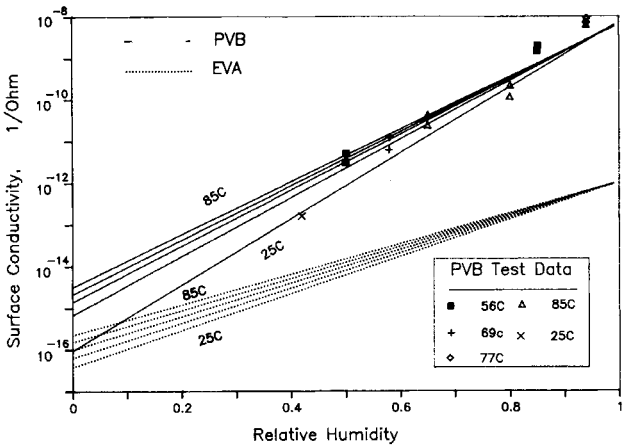

Fig. 5. Surface Conductivity of PVB and EVA

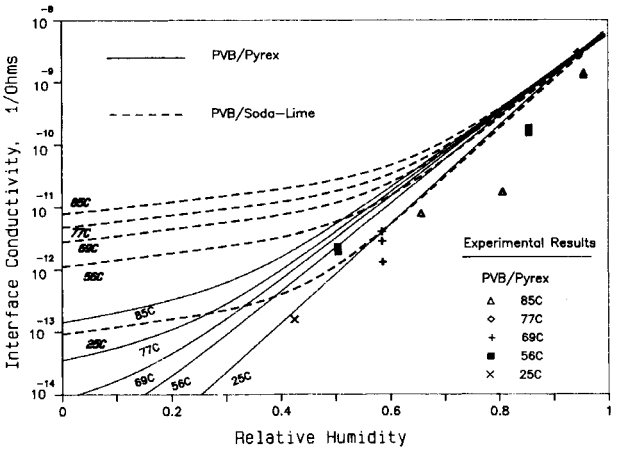

Fig. 7. Interface Conductivity, PVB/glass

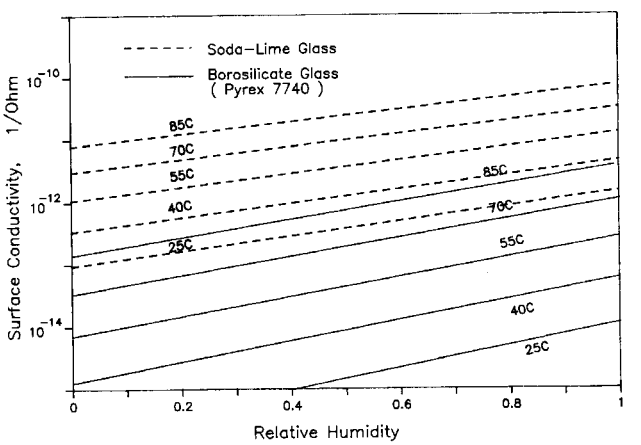

Fig. 6. Surface Conductivity of Two Glasses

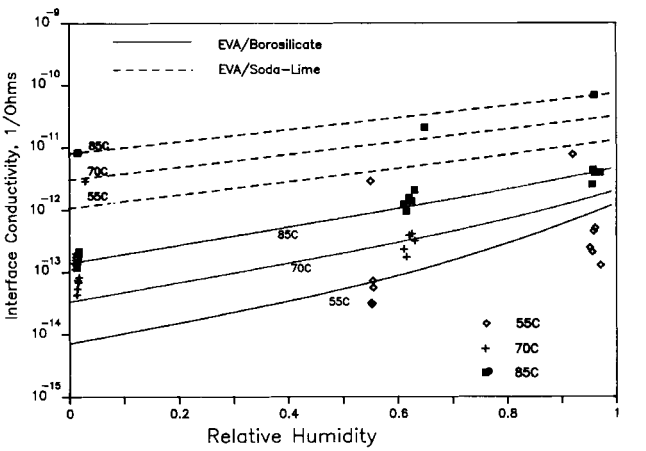

Fig. 8. Interface Conductivity, EVA/glass

The surface conductivities of borosilicate (Pyrex 7740) and soda-lime glass are presented in Fig. 6 (borosilicate glass: M_S = 23.22 ohm^{-1}, E_S = 23.3 kcal/mole, y = 0.11; soda-lime glass: M_S = 0.02775 ohm^{-1}, E_S = 15.46 kcal/mole, y = 0.11). The surface conductivity of borosilicate glass is considerably lower than that of soda-lime glass. The surface conductivity of both glasses is more sensitive to temperature variation than that of the two polymers.

Interface Conductivities. PVB/glass interface data are presented in Fig. 7 and EVA/glass interface data in Fig. 8. Evidently for PVB/glass, at low humidity the glass surface dominates, while at high humidity the PVB surface dominates, the interface conduction process. The glass surface dominates the EVA/glass interface conduction process at all humidity levels.

Additional borosilicate/polymer interface conductivity measurements were made with various polymers, including polyvinyl chlorides, fluorides, acrylics, and polyesters. The glass dominated the interface conduction process for all but the polyester/glass composite.

Experimental Results: Field

The same samples that were used to obtain the laboratory bulk, surface, and interface leakage current measurement data were then field mounted at a JPL outdoor test site. Raw data collected over four different days in March 1986 are presented as bulk, surface, and interface leakage currents in Figs. 9 - 11, respectively. Beneath the data for each day, the type of day is indicated by a typifying word and temperature. To the left of the field data, for the purpose of comparison, are the corresponding 85°C laboratory measurement data for the same samples.

General observations are that in both laboratory and field environments, currents in PVB considerably exceeded those in EVA, interface currents exceeded surface currents, and large surface and interface current excursions occurred during periods of rain and dew.

The fact that these low temperature field data have associated with them current levels comparable to and exceeding those observed in what is considered to be a severe accelerated

environment--namely, 85°C/100%RH--underscores the major role liquid water plays in establishing field leakage current levels and hence in contributing to PV module electrochemical corrosion. Indeed, when doing life prediction simulation, it may suffice to consider only the leakage currents generated during periods of module exposure to liquid water.

One form of water damage actually observed at the test-stand was the formation of liquid water pockets at material interfaces of some test coupons. As temperature increased, this trapped water presumably vaporized, causing blistering and delaminations.

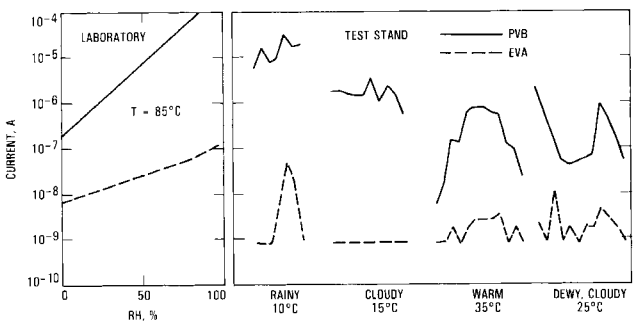

Fig. 9. Lab/Field Bulk Leakage Current Data

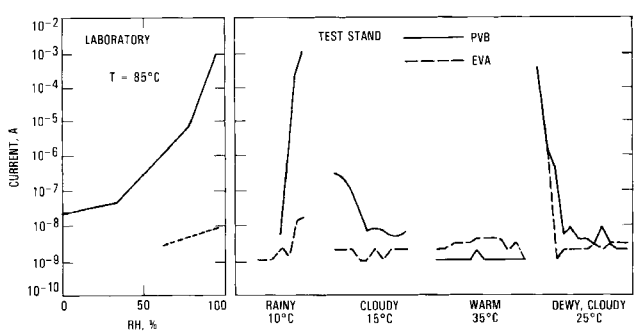

Fig. 10. Lab/Field Surface Leakage Current Data

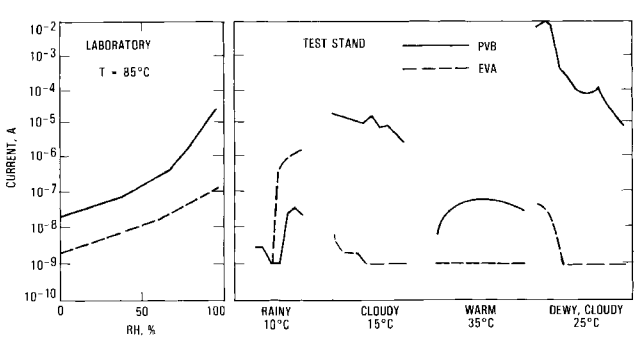

Fig. 11. Lab/Field Interface Leakage Current Data

LEAKAGE CURRENT PATHS

We now focus on the interplay of bulk, surface, and interface conductivities in determining overall conduction path geometries in PV modules. Glass superstrate test coupons were constructed consisting of a single C-Si cell and aluminum bar ("frame") encapsulated in PVB or EVA. Measurements were made at 500 volts cell-to-frame. A two-dimensional multi-nodal SINDA (11) conduction model of a typical test coupon, shown in Fig. 12, was employed to achieve a first cut understanding of leakage current division among possible paths. The ultimate parameter determining the leakage current is the total resistance R_T between cell and frame, as determined by the series/parallel network connecting the two. Fig. 13 shows how R_T varies with bulk, surface, and interface resistivities and the key geometric parameters defined in Fig. 12. In Fig. 13, ρ_{SI} is the reciprocal sum of surface and interface conductivities.

The simulation results presented in Fig. 13 supercede those presented in Fig. 8, Reference (1), which fails to account for conduction at the encapsulant/glass interface.

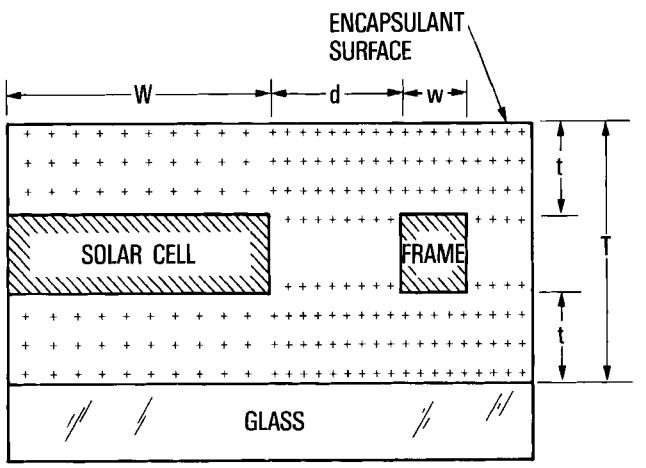

Fig. 12. Sample Model Used in Computer Conduction Simulation

In Fig. 14, the resistivity ratio (abscissa in Fig. 13) is plotted vs. temperature and relative humidity for PVB and EVA. Thus the ionic conduction characteristics generated by the simulation model (Fig. 13) can be correlated with the ionic conduction characteristics of module encapsulants in equilibrium temperature/humidity environments (Fig. 14).

As an example of the usefulness of Figs. 13 and 14, note that for EVA/glass modules the surface-interface/bulk resistivity ratio is small ($\rho_{SI}/\rho_V < 0.3$); the dominant cell-to-frame conduction paths are via the surface and interface. Under these conditions the leakage current level is inversely proportional to the encapsulant thickness t and directly proportional to the areas of the cell and frame as represented by their widths W and w, respectively, Fig. 13. This is true for PVB modules only in wet, low temperature environments, as may occur on dewy mornings or rainy days. For

PVB/glass modules in a dry environment (ρ_{SI}/ρ_V > 10.0), the conduction is dominated by lateral paths through the encapsulant bulk; the gap spacing and the total encapsulant thickness T are the governing parameters.

We point out that cells of C-Si modules are totally surrounded by insulation; hence all cell-to-frame paths have one or more bulk components. On the other hand, in a-Si modules interfacial paths directly connect the cells to the frame. The consequences of this for water entry into, and distribution within, PV modules are discussed in a companion paper (12) in this journal.

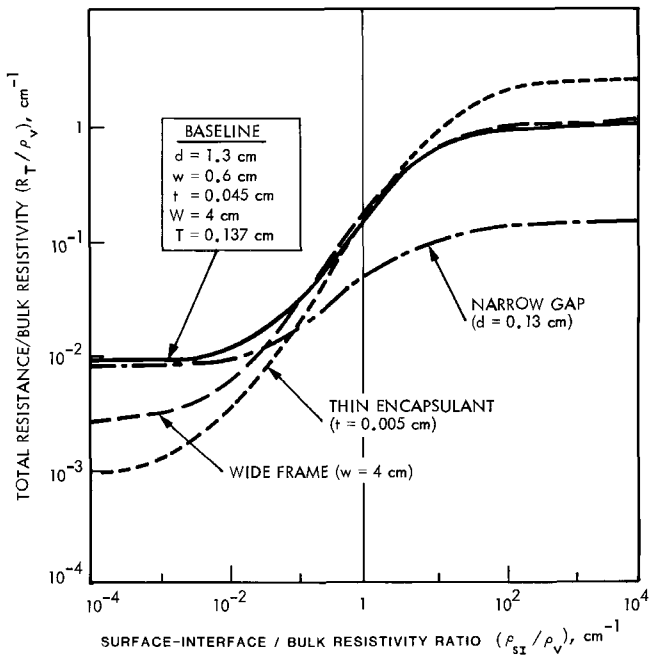

Fig. 13. Sample Ionic Conduction Characteristics

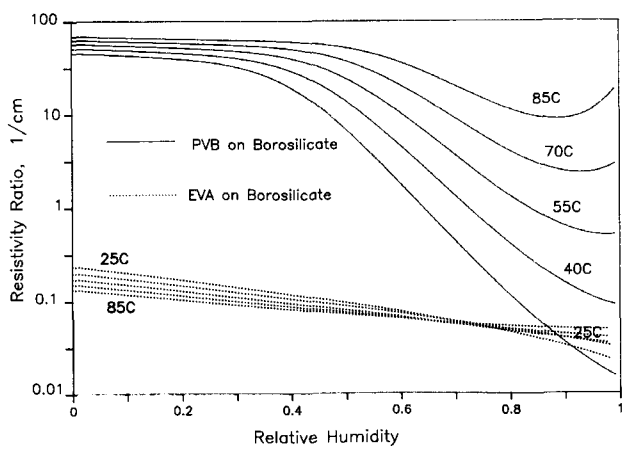

Fig. 14. Resistivity Ratios vs. Temperature and Relative Humidity

DISCUSSION AND CONCLUSIONS

In this paper we have noted the crucial role ionic leakage current plays in contributing to PV module corrosion processes. We have provided some important material ionic conduction data and have indicated how variations in module design parameters impact module leakage current levels. We have indicated likely module leakage current paths for various temperature/humidity environments and have demonstrated the greater severity of an outdoor environment over that of typical laboratory temperature/humidity test environments, emphasizing the key role of liquid water.

This paper and its antecedent (1) establish a data base and the germ of a procedure for quantitatively analyzing and predicting PV module field life. Still lacking are transient performance models that integrate the many interactive parameters into a single reliable analytical algorithm. Present transient response models are simplistic at best and a quantitative understanding of the link between the form and concentration of moisture in a polymeric material (much less a PV module), and the consequent ionic conduction and corrosion, is not now available.

ACKNOWLEDGEMENTS

The authors acknowledge Chronar Corporation for providing polymeric films, and Paul Willis of Springborn Laboratories, Inc., for providing encapsulant materials and primers for use in various JPL test programs.

The authors also recognize and appreciate the many contributions made by technicians Scott Leland and Otto Witte, and engineering assistants Elizabeth Jetter and John Meyer.

REFERENCES

1. G. Mon, L. Wen, R. Ross, Jr., D. Adent, "Effects of Temperature and Moisture on Module Leakage Currents", Proceedings of the 18th IEEE Photovoltaic Specialists Conference, October 1985, pp. 1179-1185.

2. G. Mon, G. Whitla, R. Ross, Jr., M. Neff, "The Role of Electrical Insulation in Electrochemical Degradation of Terrestrial Photovoltaic Modules", IEEE Transactions on Electrical Insulation, Vol. EI-20, No. 6, December 1985, pp. 989-996.

3. G. Mon, R. Ross, Jr., "Electrochemical Degradation of Amorphous-Silicon Photovoltaic Modules", Proceedings of the 18th IEEE Photovoltaic Specialists Conference, October 1985, pp. 1142-1149.

4. G. Mon, R. Ross, Jr., "Amorphous-Silicon Module Intercell Corrosion", Proceedings of the American Institute of Physics Conference on Stability of Amorphous Silicon Alloy Materials and Devices, Palo Alto, CA, January 1987.

5. D. Otth, R. Ross, Jr., "Assessing Photovoltaic Module Degradation and Lifetime for Long Term Environmental Tests", Proceedings of the Institute of Environmental Science, 1983 Annual echnical Meeting, Los Angeles, CA, April 19-21, 1983, pp. 121-126.

6. J.R. Martin, R.J. Gardner, Effect of Long Term Humid Aging on Plastics", Polymer Engineering and Science, V. 21, No. 9, June 1981, pp. 557-565.

7. W.F.H. Borman, "The Effect of Temperature and Humidity on the Long-Term Performance of Poly (Butylene Terephthalate) Compounds", Polymer Engineering and Science, V. 22, No.14, October 1982, pp. 883-887.

8. A.R. Blythe, "Electrical Properties of Polymers", Cambridge University Press, 1979, p. 93.

9. L. Hartshorn, N.J.L. Megson, E. Rushton, "The Structure and Electrical Properties of Protective Films", Communication No. 616, Kodak Research Laboratory, August 1937.

10. J.L. Koenig, et al., "Chemical Bonding Technology: Direct Investigation of Interfacial Bonds", JPL 5101-284, Jet Propulsion Laboratory, Pasadena, CA, January 1986.

11. J.P. Smith, SINDA User's Manual, Report No. 14690-H001-R0-00, TRW Co., 1971.

12. G. Mon, L. Wen, R. Ross, Jr., "Corrosion of a-Si Cells and Modules", this journal.